ORIGINAL ARTICLE

CrossMark

The Acute Phase of Experimental Subarachnoid Hemorrhage: Intracranial Pressure Dynamics and Their Effect on Cerebral Blood Flow and Autoregulation

Catharina Conzen[1,2] · Katrin Becker[2] · Walid Albanna[1] · Miriam Weiss[1] · Annika Bach[2] · Nyanda Lushina[2] · André Steimers[3] · Sarah Pinkernell[2] · Hans Clusmann[1] · Ute Lindauer[1,2] · Gerrit A. Schubert[1]

Abstract

Clinical presentation and neurological outcome in subarachnoid hemorrhage (SAH) is highly variable. Aneurysmal SAH (aSAH) is hallmarked by sudden increase of intracranial pressure (ICP) and acute hypoperfusion contributing to early brain injury (EBI) and worse outcome, while milder or non-aneurysmal SAH with comparable amount of blood are associated with better neurological outcome, possibly due to less dramatic changes in ICP. Acute pressure dynamics may therefore be an important pathophysiological aspect determining neurological complications and outcome. We investigated the influence of ICP variability on acute changes after SAH by modulating injection velocity and composition in an experimental model of SAH. Five hundred microliters of arterial blood (AB) or normal saline (NS) were injected intracisternally over 1 (AB_1, NS_1), 10 (AB_{10}, NS_{10}), or 30 min (AB_{30}) with monitoring for 6 h ($n = 68$). Rapid blood injection resulted in highest ICP peaks (AB_1 median 142.7 mmHg [1.Q 116.7–3.Q 230.6], AB_{30} 33.42 mmHg [18.8–38.3], $p < 0.001$) and most severe hypoperfusion (AB_1 16.6% [11.3–30.6], AB_{30} 44.2% [34.8–59.8]; $p < 0.05$). However, after 30 min, all blood groups showed comparable ICP elevation and prolonged hypoperfusion. Cerebral autoregulation was disrupted initially due to the immediate ICP increase in all groups except NS_{10}; only AB_1, however, resulted in sustained impairment of autoregulation, as well as early neuronal cell loss. Rapidity and composition of hemorrhage resulted in characteristic hyperacute hemodynamic changes, with comparable hypoperfusion despite different ICP ranges. Only rapid ICP increase was associated with pronounced and early, but sustained disruption of cerebral autoregulation, possibly contributing to EBI.

Keywords Experimental subarachnoid hemorrhage · Acute phase · Cerebral autoregulation · Early brain injury (EBI) · Intracranial pressure (ICP) · Cerebral hypoperfusion

✉ Gerrit A. Schubert
gerrit.schubert@me.com

1 Department of Neurosurgery, RWTH Aachen University, Pauwelsstr. 30, 52074 Aachen, Germany

2 Translational Neurosurgery and Neurobiology, RWTH Aachen University, Aachen, Germany

3 Institute for Occupational Safety and Health of the German Social Accident Insurance, Sankt Augustin, Germany

Introduction

Subarachnoid hemorrhage (SAH) remains an interdisciplinary treatment challenge with persistently high morbidity and mortality [1]. When caused by rupture of an intracranial aneurysm (aSAH), early mortality approaches 30%, and 30% of surviving patients develop delayed cerebral ischemia (DCI), correlating with unfavorable neurological outcome [2].

In aSAH, a plethora of experimental data as well as individual case reports suggest that aneurysm rupture followed by rapid extravasation of blood leads to a hyperacute and dramatic increase of intracranial pressure (ICP), a consecutive compromise of cerebral perfusion pressure (CPP), as well as a prolonged and CPP-independent decrease of cerebral blood

flow (CBF) [3–7]. These early changes within the first minutes after aneurysmal SAH are assumed to contribute to early brain injury (EBI) [8], an umbrella term for all acute pathological changes occurring within the first 72 h (acute vasospasm, neuroinflammation, development of microthrombi, cortical spreading depolarization, disruption of the blood–brain barrier and neuronal cell death, among others [9]), possibly also promoting the development of DCI [10]. Most importantly, early brain injury (EBI) has been identified as an important contributor to overall outcome [9, 10].

The initial clinical presentation with aSAH, however, which is thought to correlate with EBI is highly variable. The spectrum ranges from patients with mild headache to comatose patients, implying differences in hemorrhage severity and possibly also dynamics, namely ICP changes. Hemorrhage into the subarachnoid space of a confined compartment (skull) may occur rapidly, more slowly or in stages. Moreover, patients with non-aneurysmal SAH (naSAH) frequently present with a comparable amount of blood extravasation, while clinical presentation is surprisingly benign for the most part, and outcome significantly better. The underlying, yet still unproven hypothesis, is a less dramatic change in ICP in the absence of an arterial tear. Literature indicates a venous and therefore slower, oozing mechanism [11]. After SAH, variable size of the aneurysm or the respective arterial or venous tear, differences in arterial blood pressure or tamponade by surrounding parenchyma may all influence the force and dimension of the initial hemorrhage, possibly reflected by the severity of the initial neurological deficit. Consequently, the extent of EBI and development of DCI and ultimately outcome of patients may also vary. This notion is supported by the fact that acute intracranial hypertension is frequently associated with sudden loss of consciousness and worse outcome [12], a phenomenon rarely observed in patients with naSAH or mild grade aSAH. As these subcohorts of patients usually carry a significantly better prognosis, early ICP crisis and the dynamics of its alterations may therefore play an incremental part in triggering EBI as well as delayed complications.

Though the details of the delicate interplay of hyperacute changes and EBI remain controversial [5, 13, 14], cerebral autoregulation (CA) in particular is considered an integral part in the maintenance of physiological pressure dynamics. Its delayed disruption has been directly implicated in the development of DCI [15] and susceptibility for ischemic events [16, 17]. Early CA disruption in poor grade patients is suggested by some [18, 19], but only secondary deterioration of initially preserved CA has yet been reported by others [17, 20]. While interaction of abrupt intracranial hypertension, disruption of cerebral perfusion and autoregulation with EBI is conceivable, to date, there is no experimental data to substantiate the state of CA in the (hyper)acute phase of SAH and the role of ICP to trigger autoregulatory disruption.

To this end, we extended the existing cisterna-magna injection model of experimental SAH by modifying injection velocity and composition in order to emulate different ICP dynamics and their effect on immediate changes of CBF and autoregulation.

Material and Methods

Animals

A total of 68 male Wistar rats (body weight 270–340 g, Charles River, Sulzfeld, Germany) were housed specific pathogen free in species-appropriate groups for at least 1 week before surgery following a 12-h light/dark cycle with food and water ad libitum. Animal care and handling were carried out in accordance with national laws and guidelines. All experimental protocols were approved by the responsible state authorities in line with the EU Directive 2010/63/EU on the protection of animals used for scientific purposes (Landesamt für Natur, Umwelt und Verbraucherschutz (LANUV) Nordrhein – Westfalen, Recklinghausen, Germany; AZ 84-02.04.2015.A412) and were performed in accordance with the ARRIVE Guidelines [21].

Surgical Preparation

Following induction of anesthesia with 4% isoflurane in N_2O/O_2 (70:30), surgical tracheotomy was performed for mechanical ventilation and anesthesia was maintained via inhalation of 1.6–2.0% isoflurane. Body temperature was maintained at 37.5 °C via a servo-controlled heating pad (Harvard Apparatus Ltd., Kent, England). A femoral artery catheter was placed for continuous monitoring of arterial blood pressure (BLPR2 and SYS-BP1, WPI, Friedberg, Germany). For analgesia, intravenous fentanyl (0.015 mg/kg/h) was applied via a femoral vein catheter and skin cuts were additionally pretreated with local anesthesia (Ropivacain). Arterial blood gases and pH were monitored via hourly blood gas analysis (Eschweiler combi line, Eschweiler GmBH & Co KG, Kiel, Germany) and kept in physiological ranges via adaption of mechanical ventilation parameters.

Rats were placed in prone position on a stereotactic frame (Stereotaxic Frame with 18° ear bars, WPI, Friedberg, Germany). A cranial bone window was thinned out over the right parietal cortex (8 mm × 5 mm, 4 mm posteriorly from bregma, and 2.5 mm from midline) by using a drill under constant saline irrigation. The internal compact layer and dura mater were preserved to avoid loss of cerebral spine fluid during induction of SAH. The cranial window was surrounded by bone wax, filled with saline and closed with a small cover glass. For cortical electroencephalographic (cEEG) monitoring, a 1-mm burr hole was drilled 2 mm posteriorly of the cranial

window. A small silver wire was placed directly onto the dura and a reference electrode was positioned on the exposed neck musculature. The signal was filtered and amplified (gain 100, bandpass filter 0.1–1000 Hz, notch 50; amplifier 1902, Science Products, Hofheim, Germany). For ICP monitoring, a fluid-filled microcatheter, connected to a pressure transducer and monitor (BLPR2 and SYS-BP1, WPI, Friedberg, Germany), was placed in the subarachnoid space via puncture of the atlantooccipital membrane. Finally, a 1-mm burr hole was drilled 5 mm posteriorly from lambda overlying the cisterna magna. After sharp incision of the dura, a microcatheter was placed in the cisterna magna (see Fig. 1b). Five hundred micro-liters of autologous arterial blood was withdrawn from the fem-oral artery and stored in a heparinized syringe (80 IU, PICO50, Radiometer Medical ApS, Brønshøj, Denmark).

Experimental Design

To study the influence of initial ICP dynamics, we designed three arterial blood (AB) injection groups by variation of in-jection velocity of identical blood volume (500 μl), the basic principle is described elsewhere [22] choosing a comparative-ly large volume for injection in order to elicit severe SAH. With animals being assigned randomly by lot drawing, groups were designed as follows: injection of 500 μl autologous ar-terial blood over 1 min (AB_1, $n = 16$), injection of 500 μl arterial blood over 10 min (AB_{10}, $n = 12$), and injection of 500 μl arterial blood over 30 min (AB_{30}, $n = 9$). Beside these prespecified injection periods of 1 min and 10 min, the third group was designed to achieve an ICP course completely lacking the dramatic peak increase within the first minutes occurring in the other two groups, but reaching comparably delayed plateau values of 30–40 mmHg after the initial phase. Based on our experiences in the initial experiments, we found that a standardized injection time of 30 min was suitable to yield the designated ICP plateau value. These first experi-ments are included in the analysis because identical proce-dures were performed.

To study the effect of fluid composition, two normal saline injection groups completed the study design: injection of 500 μl normal saline over 1 min (NS_1, $n = 11$) and over 10 min (NS_{10}, $n = 13$). Nine animals served as time controls without injection (sham surgery). Our pilot experiments of NS_{10} showed a very small effect on the recorded parameters, so we decided to waive on an additional NS_{30} group, were even less changes due to the slower injection velocity were expected.

Monitoring

Animals remained positioned under a superficial tissue imag-ing system for analysis of microcirculation by laser speckle contrast analysis (Superficial Tissue Imaging System, STIS,

provided by Steimers et al., Biomedical Optics Laboratory, RheinAhrCampus Remagen, Germany, [23]) throughout the experiment. After 30 min of baseline recording, 500 μl blood or saline were injected into the cisterna magna over above-mentioned, prespecified time frames according to group as-signment. Injection over 10 min and 30 min was controlled using a programmable single syringe pump (NE-300 TM sy-ringe pump, New Era Pump Systems, Inc., Farmingdale, USA). Successful injection was confirmed by increase in ICP, a simultaneous reaction of CBF and a reduction of the amplitude of cEEG (see Fig. 4, suppl. material).

Rats were kept in stable anesthesia while data recording was performed for 360 min after injection. To prevent dehy-dration, rats received intravenous fluid infusion (normal sa-line) via femoral vein catheter. During the recording phase, ICP and mean arterial blood pressure (ABP), and cEEG were continuously monitored and recorded at a frequency of 1 Hz (ICP and ABP) or 5 kHz (cEEG), respectively (power 1401 data acquisition interface, and Spike2 8.02, Science Products, Hofheim, Germany). For CBF analysis, laser speckle contrast images were calculated online from raw images of speckle pattern using STIS and stored at approximately 0.5 Hz for later offline calculation of CBF from speckle contrast (see Fig. 3C, suppl. material).

At the end of the measurement period, a final exsanguina-tion was conducted by withdrawing 6–10 ml of arterial blood from the femoral artery, and animals were sacrificed in deep anesthesia by injecting 2 ml of 2.5 M potassium chloride intravenously.

Qualitative Assessment of Injection

After decapitation, brains were promptly removed and high-resolution photographs were obtained to document blood dis-tribution. Photographs were analyzed to verify successful SAH by a blinded investigator according to a modified ver-sion of the SAH bleeding scale for rats [24]. The score was dichotomized into successful SAH (whole volume injected, grades 2 and 3, coverage of basal cisterns with blood, vessels visible or no longer visible, subarachnoid blood load on ven-tral parietal and temporal lobes) and no SAH (grades 0 and 1, no or minimal blood). Saline injection or no injection in the control group was rated as successful when graded as no SAH without any signs of intracerebral hematoma due to surgical failure. Cases with subdural or visible intracerebellar hemato-ma were excluded from analysis (see Fig. 1).

Immunohistochemistry

Brains were dissected into 2 mm coronal slices and fixated in 4% paraformaldehyde for 36 h, dehydrated, embedded in par-affin and cut into 2 μm sections (Leica JUNG RM2065, Leica Microsystems Holding GmbH, Wetzlar, Germany).
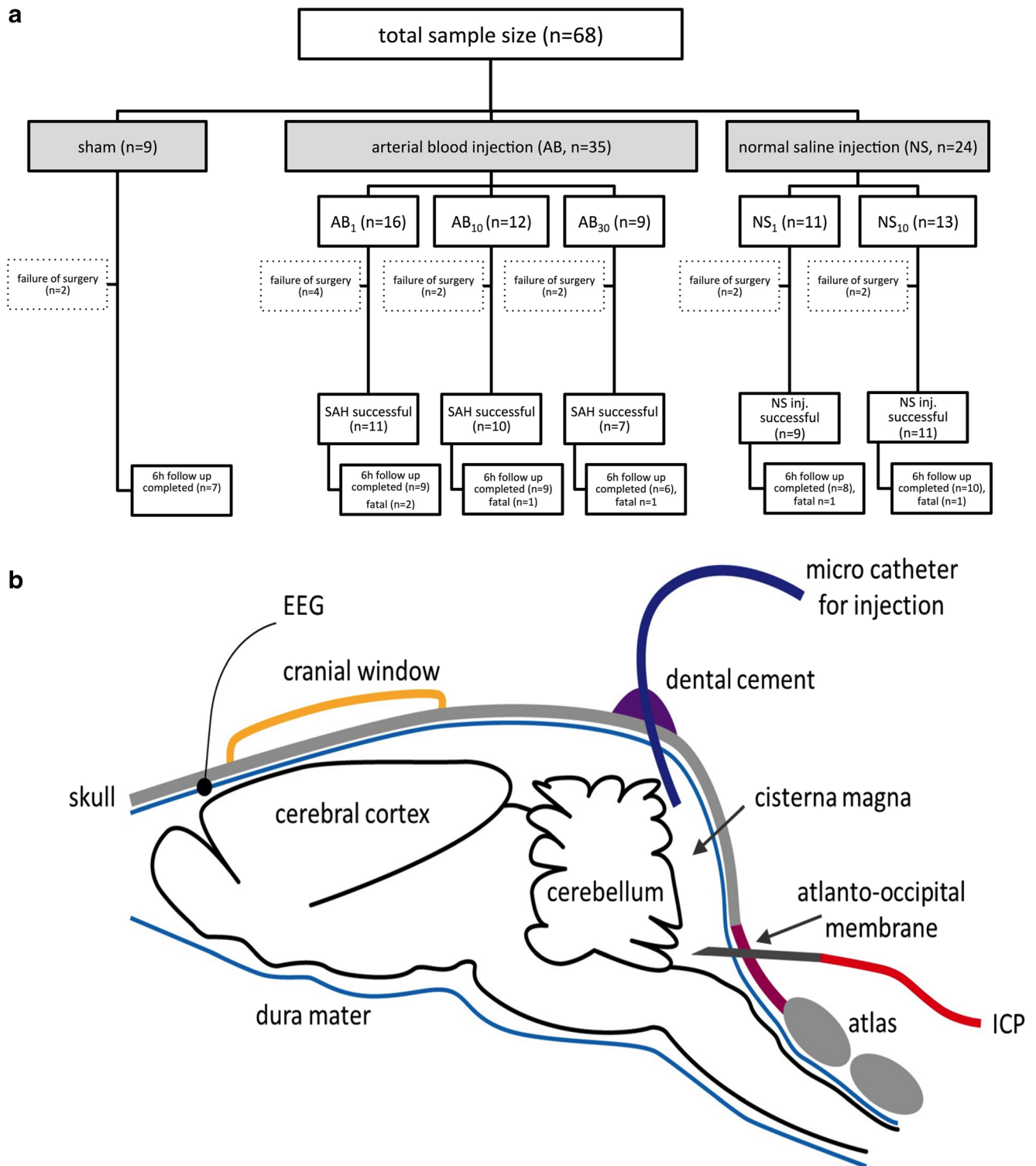
a

b

Fig. 1 Diagram of animals enrolled and experimental set up. **a** Diagram of animals enrolled: arterial blood (AB); normal saline (NS); AB1 injection of 500 μl arterial blood in 1 min, AB10 injection of 500 μl arterial blood in 10 min, AB30 injection of 500 μl arterial blood in 30 min, NS1 injection of 500 μl normal saline in 1 min, NS10 injection of 500 μl normal saline in 10 min. **b** Experimental set up in sagittal view. Illustration of the experimental setup showing the cranial window and the catheter positions for blood injection and ICP and EEG recordings

To examine incipient cell death after 6 h after SAH, immuno-fluorescence staining of neuron-specific nuclear protein (NeuN) combined with DAPI was performed. Neuroinflammation was detected by staining ionized calcium binding adapter molecule 1 (Iba1), which is specifically expressed in microglia serving as a robust biomarker for this cell type in the brain. Activated

microglial cells are morphologically characterized by cellular branches and can be easily identified. Finally, cleaved caspase-3 staining was performed to examine involvement of apoptotic signaling.

For immunofluorescence staining of NeuN, Iba1, and cleaved caspase-3, sections of treated animals (AB_1 $n = 4$, AB_{10} $n = 3$, AB_{30} $n = 3$, NS_1 $n = 3$, NS_{10} $n = 3$, control $n = 4$) were dewaxed, rehydrated, permeabilized (Triton X-100), and heated in citrate buffer (pH = 6) for antigen retrieval. After blocking in 1% phosphate-buffered saline (PBS) with 5% normal goat serum (NGS), slices were incubated over night with primary antibodies (anti-NeuN, Merck Millipore, MAB377, Darmstadt, Germany, 1:500; anti-Iba1, Abcam, Ab178847, Cambrige, UK, 1:400; anti-cleaved Caspase-3, cell signalling, 9664, 1:1000) diluted in blocking solution (1%PBS, 1% NGS). Appropriate biotinylated secondary antibodies were applied (DyLight 488 goat anti rabbit, Thermo Fisher, 35,552, Waltham, USA, 1:200 for Iba1, 1:400 for cleaved caspase-3; Alexa Fluor 555 goat anti-mouse, Thermo Fisher, A21424, Waltham, USA, 1:200 for NeuN) in PBS with 1% NGS for 1.5 h under light protection. After washing, sections were covered with Dapi Fluoromount (Southern Biotech, Cat No. 0100-20, Birmingham, USA) and sealed with cover glasses.

Immunofluorescent images were obtained with a Zeiss Axiograph 2000 (Microscope-body: Axio Imager M2; Axio Cam 506 mono; light source: HXP 120 V) using the ZEN blue edition software (2.3) and ImageJ software [25] for image acquisition and analysis. Dentate gyrus, CA3/CA4 and CA1 regions within the hippocampus and parietal cortex were assessed in both hemispheres with × 20 magnification. Immunofluorescent cells were counted and averaged in six fields in three sections of each animal by two independent, blinded investigators. The number of NeuN-positive cells was calculated as percentage of total DAPI-positive cells.

Data Processing

CBF time courses were analyzed from spatially resolved maps of speckle contrast for regions of interest within the microcirculation (see Fig. 3A+B, suppl. material) according to Steimers et al. 2013 [23] using MATLAB software (version 7.3.0.267/R2006b, The MathWorks, USA) through a blinded investigator. We analyzed all data at 0.5-Hz frequencies, with a 5-min measurement period immediately prior to injection as baseline. Cerebral perfusion pressure (CPP) was calculated from ICP and ABP according to the formula: $CPP = ABP - ICP$. Maximum increase was determined for ICP and ABP as was maximum decrease of CPP. CBF, ICP, CPP, and ABP data points were averaged over 1 min at a time to improve the signal-to-noise ratio. Artifacts resulting from temporary clotting of the arterial catheter or blood withdrawal were eliminated manually from the datasets.

Assessment of Cerebral Autoregulation

The pressure reactivity index (PRx) has been validated previously as a robust parameter for a continuous assessment of cerebrovascular autoregulation (CA) using ICP as a surrogate for cerebral blood volume [26, 27]. PRx was calculated as the moving linear Pearson correlation coefficient between ABP and ICP.

For baseline assessment, 20 consecutive frames of 60s each were analyzed and then averaged to calculate a baseline PRx as described elsewhere [26]. After injection, 30 consecutive frames of 60s each were calculated and then averaged to yield one PRx value per 30-min interval until the end of the experiment. A positive PRx of greater than 0.2 [28] indicates passive transmission of ABP waves to the cerebral blood volume resp. ICP, presuming the loss of active regulatory capacity of the cerebral vessels. A missing correlation (PRx < 0.2) indicates preserved vasomotor response, i.e., intact CA.

Statistical Analysis

A priori power analysis (free software G*Power 3.1.7) was based on previous experience with a comparable study design to estimate sample size for differentiation of parameter CBF, ICP, ABP, CA, and histological changes (power: 1-β = 0.8; α = 0.05). We included a maximum of $n = 16$ per group to account for potential dropouts. Quantitative values are presented as mean ± standard deviation (SD) or as median [1. quartile–3. quartile]. Normal distribution was tested using Shapiro–Wilk and Kolmogorow–Smirnow normality tests. Differences between two groups were analyzed using two-sided Student t test, Mann–Whitney test or chi-square test as appropriate; deviation from baseline was tested using paired t test, respectively. Comparisons between three groups were calculated with ANOVA or Kruskal–Wallis test, followed by Bonferroni's multiple comparison test or Dunn's multiple comparison test. Results are reported by p values. All analyses were performed using Numbers® (Apple Inc., Cupertino, USA) and GraphPad Prism® (GraphPad Software, Inc., La Jolla, USA). The Artwork was created using GraphPad Prism® (GraphPad Software, Inc., La Jolla, USA).

Results

A total of 68 rats were randomized and operated on; 14 animals were excluded from analysis due to anesthesia related incidents, failure of surgical preparation, or subdural or intracerebral hematoma as cerebral comorbidity. After injection, one animal from group AB_1 and AB_{30} each died immediately after injection and was excluded from analysis (see Fig. 1).

Blood gases and body temperature remained within physiological ranges throughout the surgery and observation

period (suppl. material, Table 6a and 6b). SAH was confirmed in each animal with comparable blood distribution on the basal and parietal planes. SAH was absent in all animals with NS injection or sham operation (Fig. 1, suppl material).

Intracranial Pressure

All groups showed significant increase of ICP compared to baseline after completion of fluid injection (AB_1 142.7 mmHg [116.7–230.6], $p < 0.001$; AB_{10} 72.0 mmHg [60.7–96.0], $p < 0.001$; AB_{30} 33.42 mmHg [18.8–38.3], $p < 0.001$; NS_1 70.7 mmHg [44.4–86.1], $p < 0.01$; NS_{10} 23.4 mmHg [19.3–26.2], $p < 0.001$) (Fig. 2a, b).

Within the blood injection groups, animals undergoing rapid injection (AB_1) developed the highest ICP increase (AB_1 vs. AB_{10} $p < 0.05$, AB_1 vs. AB_{30} $p < 0.001$)(Fig. 2c).

Rapid saline injection led to a significantly larger increase of ICP compared to prolonged injection (NS_1 vs. NS_{10}, $p < 0.001$). Notably, rapid blood injection (AB_1) resulted in higher absolute ICP increase than the time-equivalent saline injection (NS_1).

Maximum ICP of AB_{10} was observed after completion of injection (10 min)(AB_1 vs. AB_{10} $p < 0.05$; AB_{10} vs. AB_{30}, $p < 0.01$). There was no difference between AB_1 and AB_{30} at this time. The extent of ICP increase as measured by the area under the curve for the first hour after injection was comparable for all hemorrhage groups (n.s., data not shown).

NS_{10} showed significantly elevated ICP values compared to NS_1 after 10 min (NS_1 vs. N_{10} $p < 0.001$). After 10 min, all groups showed significantly increased ICP values compared to baseline (AB_1 $p < 0.001$, AB_{10} $p < 0.001$, AB_{30} $p < 0.01$, NS_1 $p < 0.01$, NS_{10} $p < 0.001$)(data in suppl. tables).

After 30 min, there was no detectable difference between the blood injection groups (AB_1 33.5 mmHg [18.6–39.7], AB_{10} 36.5 mmHg [18.5–41.0], AB_{30} 28.71 mmHg [20.0–37.6]; AB_1 vs. AB_{10} vs. AB_{30} $p = 0.73$) (Fig. 2c). Notably, ICP was still significantly increased compared to baseline (AB_1 $p < 0.001$, AB_{10} $p < 0.001$, AB_{30} $p < 0.01$). Rapid blood injection groups (AB_1 and AB_{10}) showed significantly elevated ICP values compared to baseline throughout the complete observation period. In AB_{30}, however, ICP was increased only for the first half of the observation period (Fig. 2a). Saline groups showed a normalization of ICP after 30 min compared to baseline (NS_1 $p = 0.24$, NS_{10} $p = 0.3$) (Fig. 2a, b).

Arterial Blood Pressure

Rapid injection groups AB_1 and NS_1 demonstrated a significant increase compared to baseline with AB_1 presenting the highest peak (AB_1 155.1 mmHg [130.3–163.4], $p < 0.001$; NS_1 111.4 mmHg [103.8–118.4]) after completed injection (Fig. 3a). NS_{10} was also associated with an increase in ABP for a shorter period (NS_{10} 91.3 mmHg [71.9–111.8]; $p < 0.05$) (Fig. 3b).

ABP increase was significantly higher in AB_1 than in the other blood injection groups (AB_1 vs. AB_{10} $p < 0.05$, AB_1 vs. AB_{30} $p < 0.001$). There was no difference between AB_{10} and AB_{30} ($p = 0.42$) (Fig. 3c, suppl. Table 3).

After 1 h, ABP returned to baseline in all groups. No significant differences between the groups occurred for the rest of the experiment (Fig. 3a, b).

Cerebral Perfusion Pressure

Following injection, a significant decrease in CPP compared to baseline was observed in all blood injection groups ($p < 0.001$)(Fig. 4a). AB_1 presented the lowest CPP (AB_1 0 mmHg, AB_{10} 17.9 mmHg, AB_{30} 30.1 mmHg)(Fig. 4a, c) and a prolonged, significant decrease until the end of the observation period compared to the baseline (approx. 40 mmHg at 350 min, $p < 0.01$). In AB_{10} and AB_{30}, a faster recovery of CPP occurred (approx. 60 mmHg after 120 min). CPP remained significantly decreased in AB_{10} for 240 min ($p < 0.05$) and in AB_{30} for 120 min ($p < 0.05$) compared to the baseline (Fig. 4a, c, suppl. Table 2). Saline injection did not influence CPP (Fig. 4b).

Cerebral Blood Flow

In all AB groups, blood injection resulted in a highly significant decrease of CBF compared to baseline (AB_1 $p < 0.001$; AB_{10} $p < 0.001$; AB_{30} $p < 0.001$) (Fig. 5a, c; suppl. Table 1). Hypoperfusion was most pronounced in the rapid injection group AB_1 (AB_1 16.6% of baseline (%) [11.3–30.6]; AB_{10} 43.2% [27.4–64.9] AB_{30} 44.2% [34.8–59.8]; AB_1 vs. AB_{10} $p < 0.05$; AB_1 vs. AB_{30}, $p < 0.05$; AB_{10} vs. AB_{30} ns) (Fig. 5a, d). Absolute minimum of CBF was reached upon completion of injection in each group: 1.5 min [1.1–2.0] after start of injection in AB_1, at 12.1 min [10.9–45.8] in AB_{10}, and at 33.4 min [30.4–43.3] in AB_{30} (AB_1 vs. AB_{10} $p < 0.01$, AB_1 vs. AB_{30} $p < 0.001$, AB_{10} vs. AB_{30} ns) (Fig. 5a). In contrast, NS injection resulted in an immediate, significant CBF increase in both groups (NS_1 143.5% [118.8–154.4]; NS_{10} 120.7% [113.0–142.1]; NS_1 $p < 0.01$, NS_{10}, $p < 0.01$; NS_1 vs. NS_{10} $p = 0.18$) (Fig. 5b).

After 10 min, CBF was still significantly decreased compared to baseline in AB_1 and AB_{10} (AB_1 73.0% [56.6–79.5], $p < 0.01$; AB_{10} 68.0% [32.1–90.8], $p < 0.01$) without any intergroup differences ($p = 0.99$). AB_{30} showed a non-significant decrease compared to baseline after 10 min ($p = 0.29$) and CBF was higher compared to AB_1 ($p < 0.05$) (Fig. 5a, d). Solely in NS_{10}, CBF was significantly increased compared to baseline after 10 min (NS_{10} 105.6% [102.9–122.3], $p < 0.01$), returning quickly to baseline thereafter throughout the rest of the experiment.
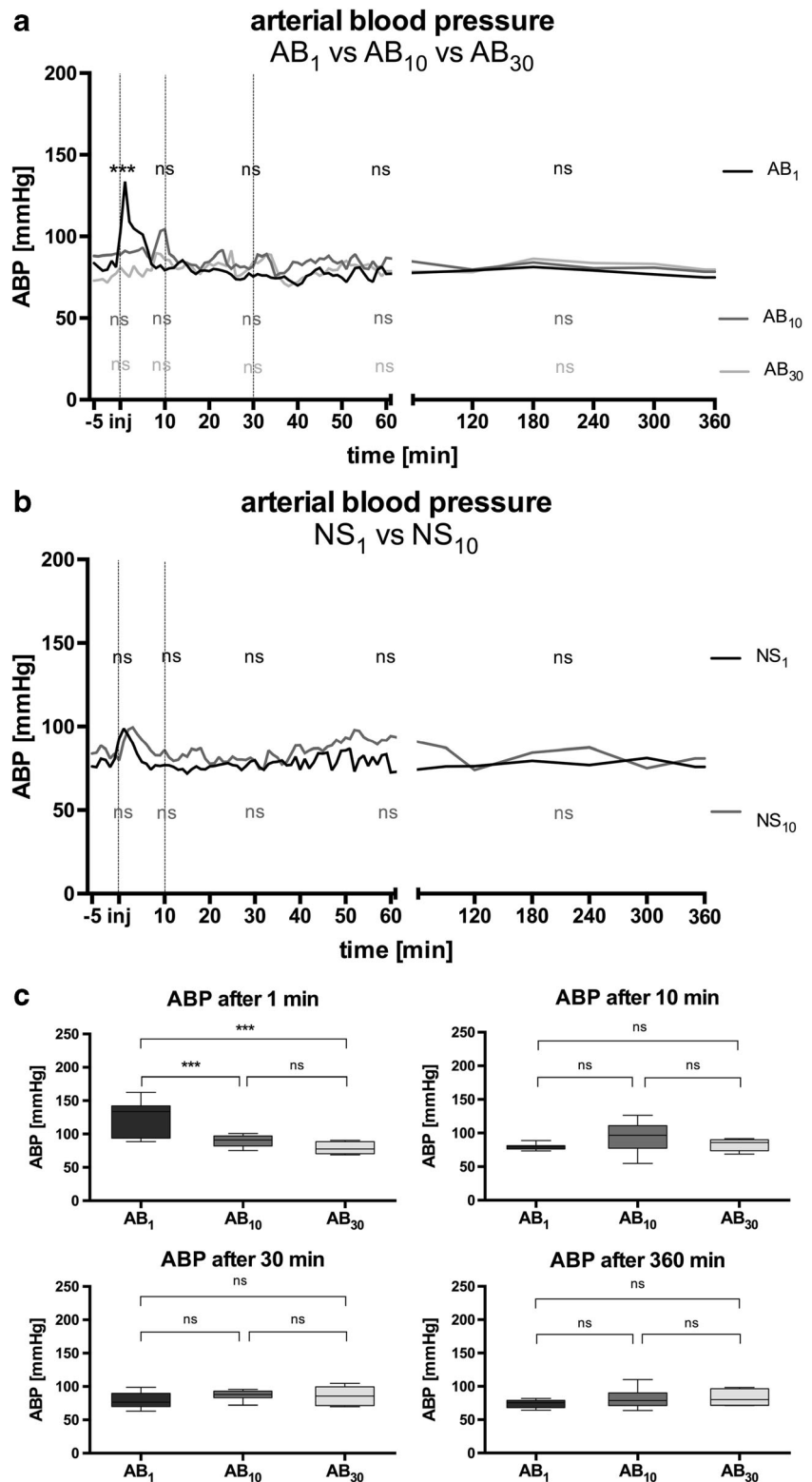
Fig. 2 Course of intracranial pressure (ICP) in all groups. **a** Course of ICP of blood injection groups. Graphs demonstrate statistical differences from baseline per group. **b** Course of ICP of saline injection groups. Graphs demonstrate statistical differences from baseline per group. **c** Figure of boxplots comparing all three blood injection groups at different time points: 1 min, 10 min, 30 min, 360 min. Arterial blood (AB); normal saline (NS); AB1 injection of 500 μl arterial blood in 1 min, AB10 injection of 500 μl arterial blood in 10 min, AB30 injection of 500 μl arterial blood in 30 min, NS1 injection of 500 μl normal saline in 1 min, NS10 injection of 500 μl normal saline in 10 min (***$p < 0.001$; **$p < 0.01$; *$p < 0.05$; ns $p > 0.05$)
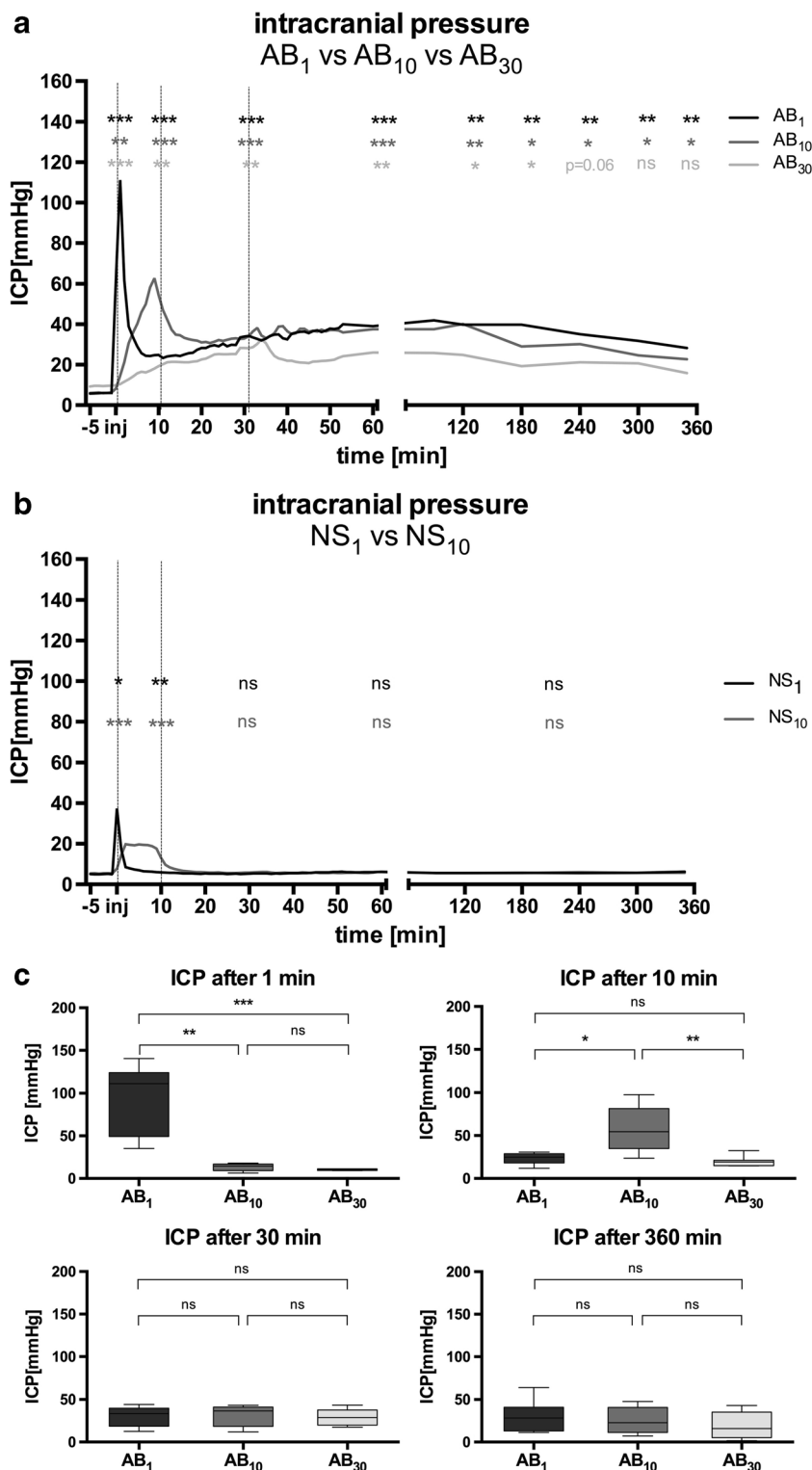

After 30 min, CBF remained significantly decreased compared to baseline in all blood injection groups (AB$_1$ 65.4% [52.1–79.3], $p < 0.01$; AB$_{10}$ 63.8% [47.4–75.0], $p < 0.001$; AB$_{30}$ 60.9% [52.6–71.3], $p < 0.01$) without intergroup differences. In AB$_1$, hypoperfusion outlasts for 120 min compared to baseline. AB$_{10}$ and AB$_{30}$ showed a prolonged decrease for 240 min, approaching baseline thereafter. NS groups showed no change in perfusion after the hyperacute increase. Representative images of CBF of the AB groups at relevant time points illustrate the described quantifications (Fig. 5c).

Fig. 3 Course of arterial blood pressure (ABP) in all groups. **a** Course of ABP of blood injection groups. Graphs demonstrate statistical differences from baseline per group. **b** Course of ABP of saline injection groups. Graphs demonstrate statistical differences from baseline per group. **c** Figure of boxplots comparing all three blood injection groups at different time points: 1 min, 10 min, 30 min, 360 min. Arterial blood (AB); normal saline (NS); AB1 injection of 500 μl arterial blood in 1 min, AB10 injection of 500 μl arterial blood in 10 min, AB30 injection of 500 μl arterial blood in 30 min, NS1 injection of 500 μl normal saline in 1 min, NS10 injection of 500 μl normal saline in 10 min (***$p < 0.001$; **$p < 0.01$; *$p < 0.05$; ns $p > 0.05$)

Cerebral Autoregulation

CA was intact in all groups before injection. AB_1 and AB_{10} showed significant disruption of CA acutely ($p < 0.05$; average 15–20 min), followed by rapid normalization. A secondary worsening of CA was observed in AB_1, which then persisted throughout the observation period. AB_{10} showed a fluctuating course, intermittently exceeding the critical threshold of PRx > 0.2.

Fig. 4 Course of cerebral
perfusion pressure (CPP) in all
groups. **a** Course of CPP of blood
injection groups. Graphs demon-
strate statistical differences from
baseline per group. **b** Course of
CPP of saline injection groups.
Graphs demonstrate statistical
differences from baseline per
group. **c** Figure of boxplots com-
paring all three blood injection
groups at different time points:
1 min, 10 min, 30 min, 360 min.
Arterial blood (AB); normal sa-
line (NS); AB1 injection of 500 µl
arterial blood in 1 min, AB10 in-
jection of 500 µl arterial blood in
10 min, AB30 injection of 500 µl
arterial blood in 30 min, NS1 in-
jection of 500 µl normal saline in
1 min, NS10 injection of 500 µl
normal saline in 10 min (***$p <$
0.001; **$p < 0.01$; *$p < 0.05$; ns
$p > 0.05$)
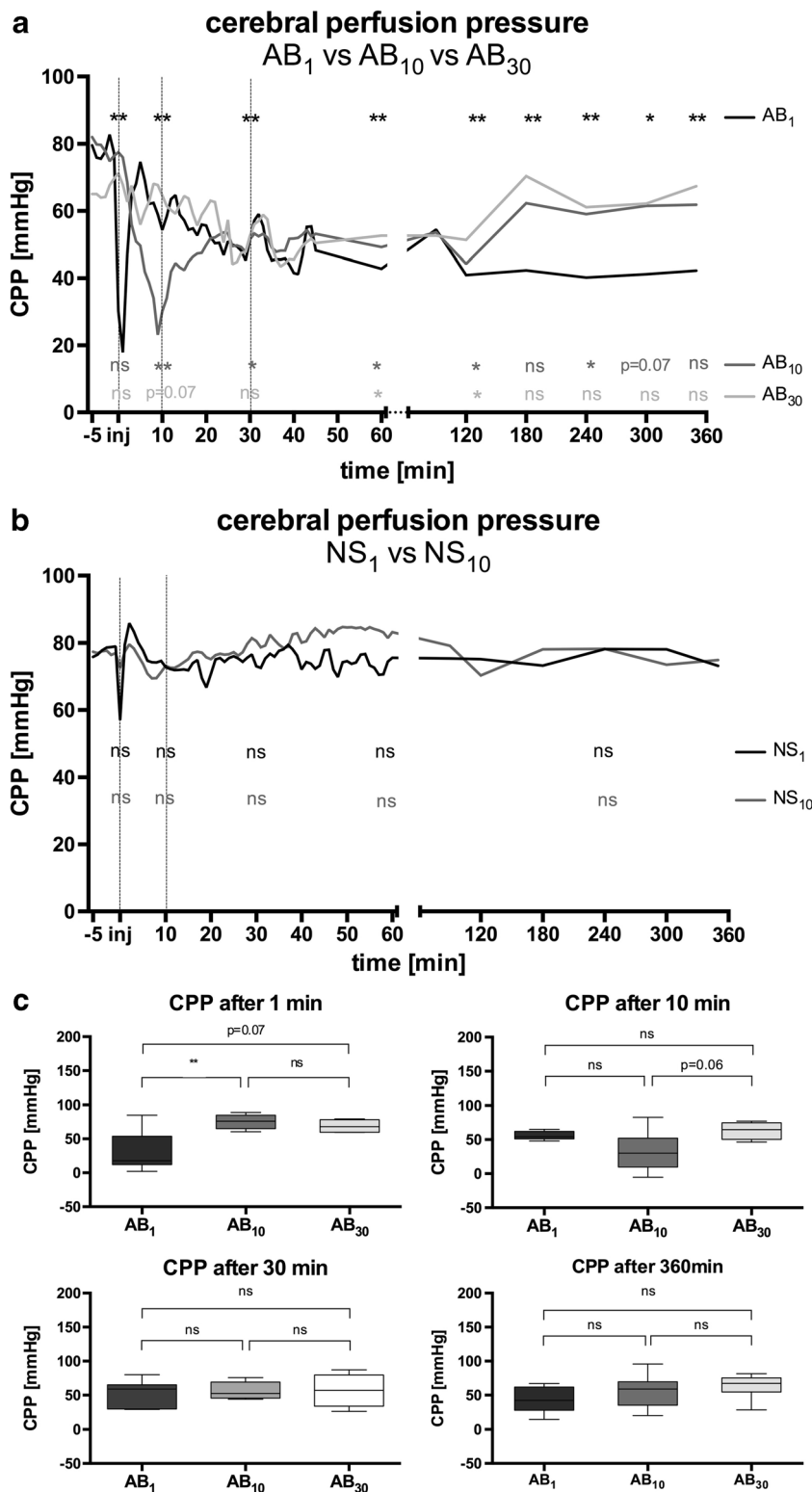
In AB$_{30}$, PRx was preserved initially, but disruption
of CA occurred upon completion of injection ($p <$
0.001) followed by recovery thereafter. Afterwards,
PRx returned to a normal range for the rest of the

observation period (Fig. 6a). NS$_1$ showed an acute,
though non-significant increase in PRx ($p = 0.07$), with
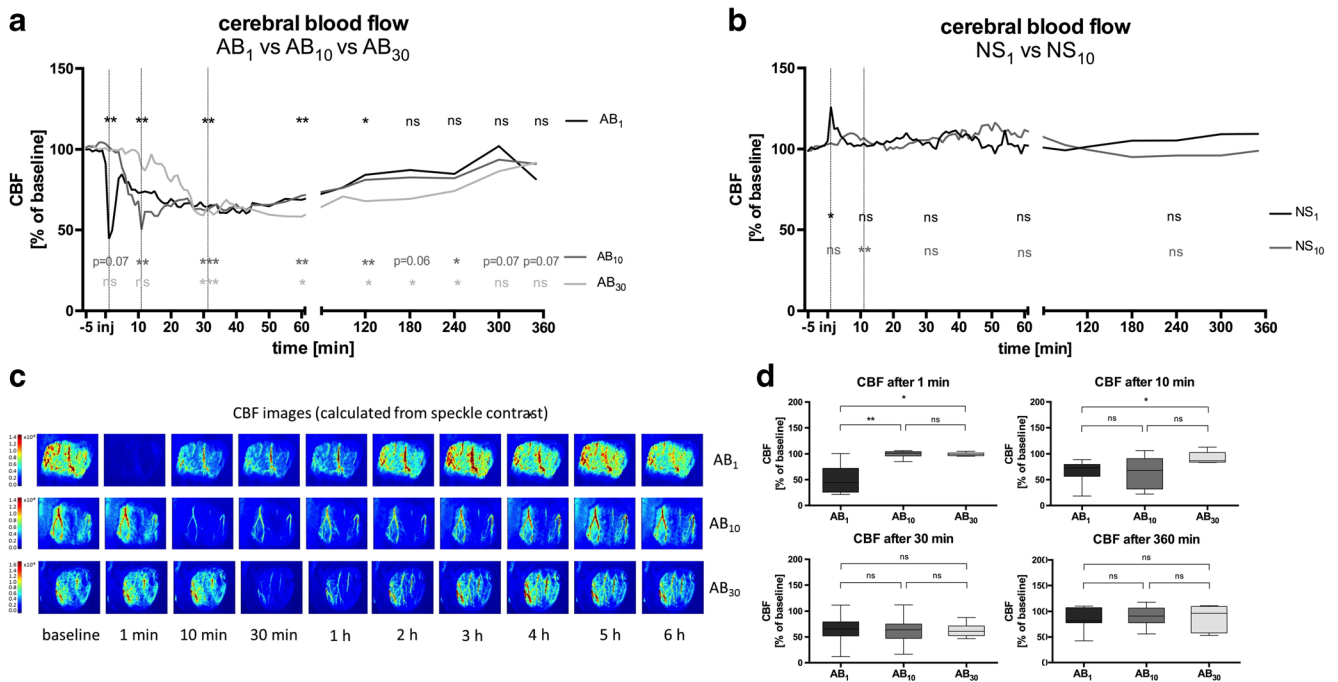fast recovery after 30 min. PRx was unaffected in NS$_{10}$
(Fig 6b).

Fig. 5 Course of cerebral blood flow (CBF) in all groups. **a** Course of CBF of blood injection groups. Graphs demonstrate statistical differences from baseline per group. **b** Course of CBF of saline injection groups. Graphs demonstrating statistical differences from baseline per group. **c** Representative images of CBF (calculated for laser speckle contrast images) of blood injection groups at relevant time points of the quantitative analysis. **d** Figure of boxplots comparing all three blood injection groups at different time points: 1 min, 10 min, 30 min, 360 min. Arterial blood (AB); normal saline (NS); AB1 injection of 500 μl arterial blood in 1 min, AB10 injection of 500 μl arterial blood in 10 min, AB30 injection of 500 μl arterial blood in 30 min, NS1 injection of 500 μl normal saline in 1 min, NS10 injection of 500 μl normal saline in 10 min (***$p < 0.001$; **$p < 0.01$; *$p < 0.05$; ns $p > 0.05$)

Immunofluorescence

The number of NeuN+ cells in the dentate gyrus was reduced in the rapid injection group (AB1 vs. AB10 $p < 0.05$ AB1 vs. control $p < 0.05$). With NS injection, no significant reduction of NeuN+ cells was detectable ($p = 0.99$) (Fig. 7).

In CA3/CA4, CA1 and parietal cortex, no difference in NeuN+ cell quantities was detectable between the blood injection groups compared to the control group ($p = 0.63$).

In CA1, the rapid NS injection group showed a reduced number of NeuN+ cells compared to NS10 ($p < 0.05$) and to the control group ($p < 0.05$).

Further statistical analysis of the dentate gyrus, CA3/CA4, CA1 and parietal cortex revealed no statistical differences regarding Iba1+ cells between groups except for NS1 showing less Iba1 cells than NS10.

Analysis of cleaved caspase-3 staining revealed no positive signaling in any group (data not shown).

Discussion

Even with comparable amount and distribution of blood in the subarachnoid space, clinical presentation and course of SAH are highly variable, as are the chances for good neurological outcome [29–32]. This phenomenon may in part be explained by divergent pathophysiological dynamics in the acute phase during and early after blood extravasation.

Beside the mostly mildly affected patients with naSAH [32], even for patients with frank aneurysmal SAH great variability of initial neurological compromise is observed. Clinicians observe a broad spectrum from mildly affected patients without signs of raised ICP (and usually good prognosis) to patients with initial loss of consciousness, generally attributed to transient global ischemia secondary to a massive intracranial hypertensive crisis and consecutive, though short perfusion arrest. Due to the delay in presentation and limited availability of acute ICP recordings, robust clinical data about the actual changes immediately after SAH is lacking.

Given the possible role for ICP changes in dictating the severity of EBI, we modified an existing experimental model to account for variable dynamics, namely the velocity of hemorrhage and its composition and to investigate the downstream cascade of pathophysiological mechanisms in the acute phase after SAH.

Effects of Injection Velocity on ICP, ABP, CPP, and CBF

Variation of injection velocity of comparable blood volume into cisterna resulted in characteristic differences regarding the
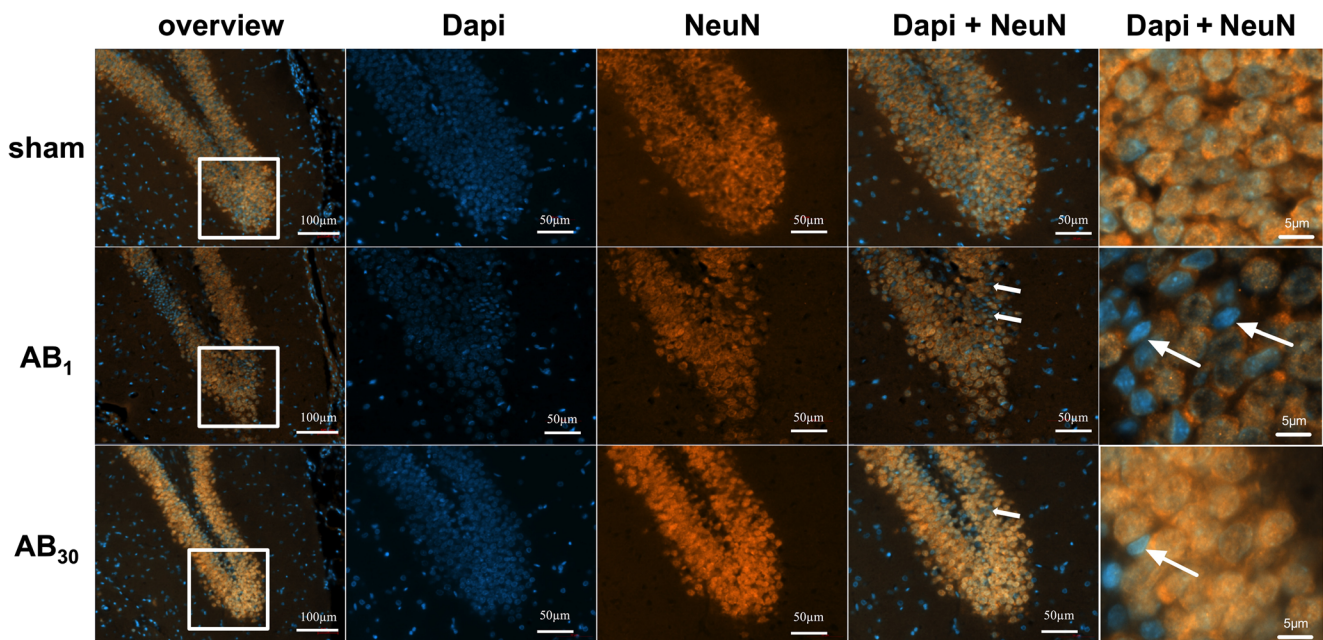
a

autoregulation (PRx) of AB_1, AB_{10} and AB_{30}

b

autoregulation (PRx) of NS_1, NS_{10} and control
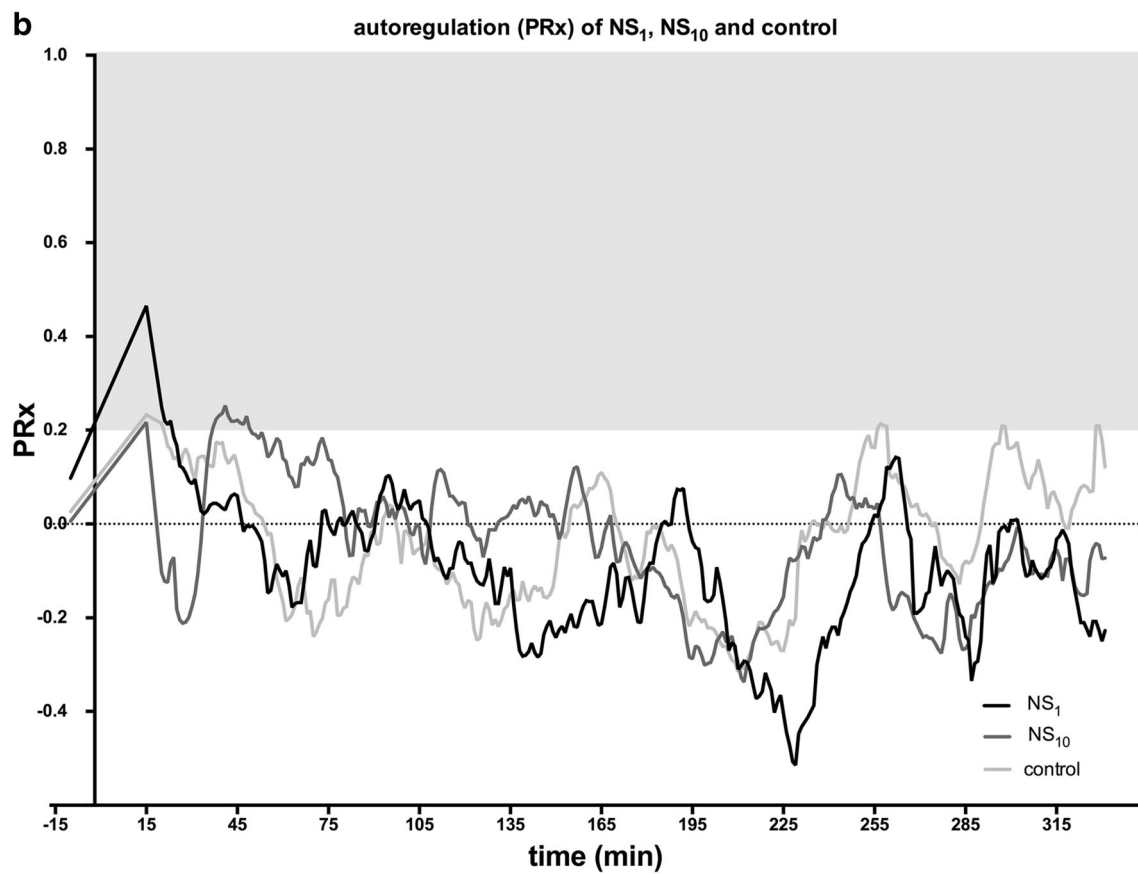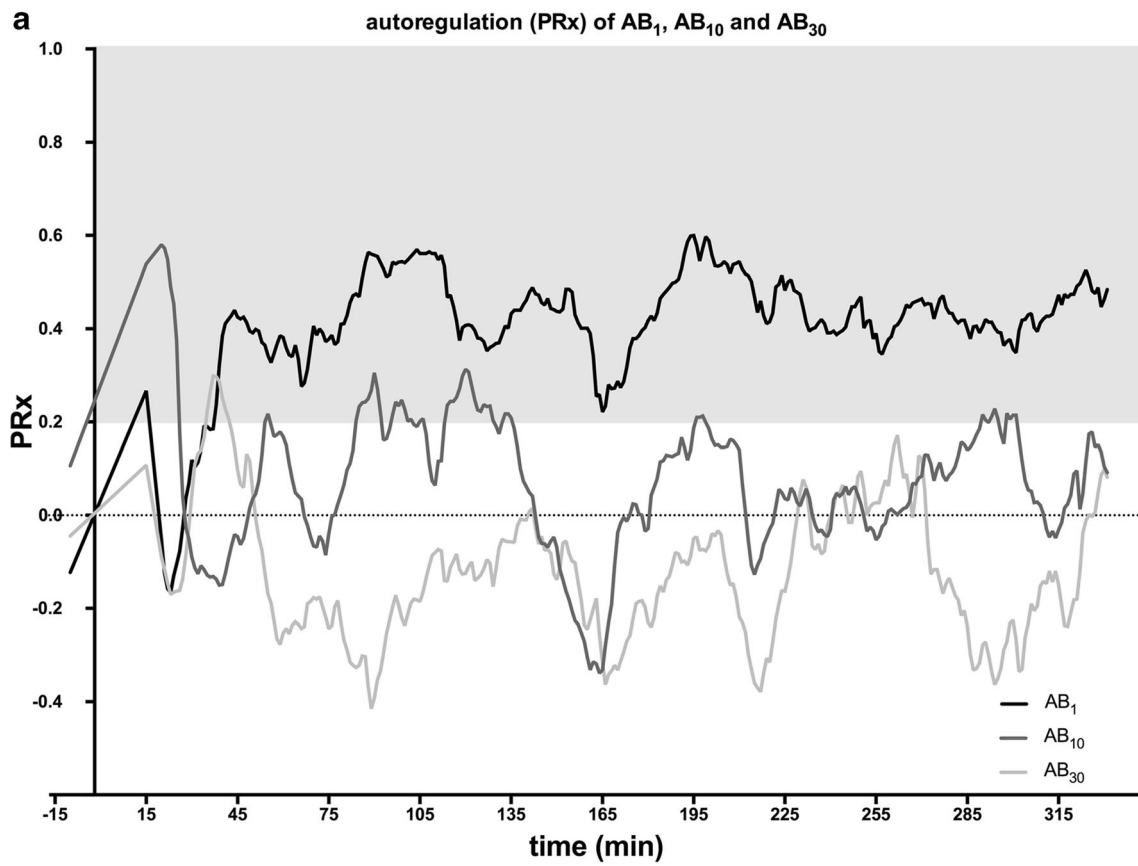
Fig. 7 Early neuronal cell loss in dentate gyrus. NeuN and Dapi staining of dentate gyrus 6 h after SAH. Pronounced neuronal cell loss in rapid blood injection group (white arrows mark dead cells). Arterial blood (AB); AB1 injection of 500 µl arterial blood in 1 min, AB30 injection of 500 µl arterial blood in 30 min, sham = control

dynamics of ICP increase, both in terms of onset and maximum values. While rapid injection of blood led to a steep rise of ICP with higher maximum peaks, a prolonged injection created a slower rise of ICP with significantly lower ICP peaks. After completion of the injection, however, a comparable elevation of ICP was observed throughout the rest of the experiment irrespective of injection velocity.

Accordingly, the rapid blood injection group demonstrated a rapid decrease of CPP with global, though transient perfusion arrest, paralleled by a rapid increase in ABP. This could be interpreted as a Cushing reflex to maintain an adequate CPP in case of rapid ICP increase [33]. A significant increase in arterial blood pressure was only observed in the experimental group with the highest, acute ICP increase (AB$_1$) and led to a transient restoration of CBF after the initial, hyperacute decrease.

◀ **Fig. 6** Course of pressure reactivity index (PRx) in all groups. The pressure reactivity index (PRx) was calculated as the moving linear Pearson correlation coefficient between ABP and ICP. A positive PRx of greater than 0.2 indicates passive transmission of ABP waves to the cerebral blood volume resp. ICP, presuming loss of active regulatory capacity of the cerebral vessels. A missing correlation (PRx < 0.2) indicates preserved vasomotor response, i.e., intact cerebral autoregulation. **a** Course of PRx of blood injection groups. Gray area indicates pathological values > 0.2. **b** Course of PRx of saline injection groups and control group. Gray area indicates pathological values > 0.2. Arterial blood (AB); normal saline (NS); AB1 injection of 500 µl arterial blood in 1 min, AB10 injection of 500 µl arterial blood in 10 min, AB30 injection of 500 µl arterial blood in 30 min, NS1 injection of 500 µl normal saline in 1 min, NS10 injection of 500 µl normal saline in 10 min (***$p < 0.001$; **$p < 0.01$; *$p < 0.05$; ns $p > 0.05$)

Literature recommends a CPP above 70 mmHg after traumatic brain injury for favorable outcome [34], and there is growing evidence, that after SAH, an individualized optimal CPP might be helpful for maintaining CBF and CA [35]. In our setting, all blood injection groups showed a reduced CPP below the critical threshold for the first 2 h. However, only the rapid blood injection group featured a prolonged compromise in CPP until the end of the observation period suggesting a persistent effect in line with the severity of the initial, intracranial hypertensive crisis.

To study the pure volume effect of the injection irrespective of its composition, we implemented two groups undergoing saline instead of blood injection over predefined time frames. Rapid saline injection led to a short, but less pronounced increase of ICP, also with mild and statistically non-significant, concordant increase in ABP (see above). Furthermore, ICP values returned to baseline rapidly after injection, while neither rapid nor slow normal saline injection influenced CPP.

Early hypoperfusion due to acute vasoconstriction is an established phenomenon after SAH [7, 36]. It is more pronounced in high-grade SAH patients, but also occurs in less severely affected patients [3, 4]. There are experimental data investigating the severity of hemorrhage dictated by the amount and location of blood injected [5, 37–39]. Distinct dynamics of ICP changes and their direct influence on perfusion pressure, CBF and CA—which may vary considerably for instance in aSAH and naSAH—are less clear. Partial preservation of CBF and CA in the acute phase could be considered a plausible explanation for less pronounced EBI and better outcome.

After rapid injection, following the transient restoration of CBF due to the increase of ABP, we observed a secondary deterioration and a longer recuperation period for CBF. Slower injection, however, was associated with a slower decrease of CBF starting shortly after injection. Remarkably, once the whole blood volume was injected (after 10 and 30 min, respectively), CBF was significantly and comparably reduced in all hemorrhage groups regardless of the injection velocity and divergent ICP dynamics.

This indicates an acute compromise in CBF after SAH probably caused by acute vasoconstriction independent from CPP and ICP as demonstrated before [3–7, 13, 40]. Others showed that a rapid and large increase of ICP leads to more pronounced acute CBF reduction and cell death [38], while some report an equal contribution of initial ICP increase and the extravasated subarachnoid blood per se [41]. Most study designs, however, lack a volume control. With this study, we examined the effects of different ICP dynamics created by injecting equal blood volumes at different velocities. Our results are in line with the reported pressure-independent phenomenon of cerebral hypoperfusion and emerge evidence that acute perfusion changes outlast ICP and CPP changes even in a volume controlled setting.

Injection of normal saline resulted in transient hyperperfusion also reported by other groups [5]. In addition to the effect of a (mild) Cushing reflex in response to the increase in ICP, moderate hyperperfusion respectively cerebral vasodilatation may be associated with the acidic properties of normal saline because acid-base regulation is known to influence cerebrovascular tone [42]. Others showed a comparable ICP increase and CBF decrease between blood and normal saline [36], but smaller volumes and different injection technique impede the comparison. Our data challenge using normal saline injection as the ideal control group. We observed fundamental differences regarding ICP peak and plateau, reaction of ABP and CPP and hyperperfusion instead of hypoperfusion despite identical volumes and injection velocity. We postulate, that due to its crystalloid characteristics, normal saline translocated more quickly from the cisterna magna, possibly into the spinal canal. Finally, the glymphatic system of the brain, a network of paravascular tunnels through which cortical interstitial solutes are cleared from the brain by translocation into the paravascular space and then to the lymphatic system of the dura [43], may be impaired by subarachnoid hemorrhage either directly though adhesions or even indirectly by cortical spreading depolarization that have been shown to close the perivascular space [43]. Hypothetically, this may be another reason for the prolonged increase of ICP after injection of autologous blood. On the other hand, saline may easily been cleared along the paravascular space into the lymphatic system resulting in a smaller and only transiently increased ICP.

Pilot experiments using colloid fluids for injection were initiated, and first preliminary data show promising results

with higher ICP peaks and a longer lasting ICP plateau throughout the observation period (data not shown). Future experiments accounting for higher viscosity may help to substantiate our findings.

Cerebral Autoregulation in the Acute Phase After Subarachnoid Hemorrhage

Physiologically, vessel diameter is constantly adapted by regulating mechanisms acting at global and regional levels—a compensatory, autoregulatory function known to be impaired several days after aSAH [18]. Sustained CA impairment is associated with development of DCI and poor neurological outcome [15, 18, 20]. Data concerning acute phase alterations of CA are sparse and non-existent for the first minutes to hours after SAH. Recently, impairment of other important cerebral perfusion regulating mechanisms such as neurovascular coupling and reactivity to CO_2 has been demonstrated several hours after hemorrhage [44, 45]. So far, impaired CA has been associated with suppressed vasomotor adaptability [36, 46]. Others demonstrated that SAH changes the range of CA after 48 h [47]. Using PRx, a common index for cerebral CA, we investigated CA in our volume-controlled setting in the acute phase after SAH. With injection, PRx exceeded the pathological threshold initially in both rapid blood injection groups and the rapid saline injection group. We interpreted these changes to be connected to the Cushing reflex in the context of rapid ICP and ABP increase beyond the autoregulatory range, followed by fast recovery of PRx to baseline thereafter. PRx of the normal saline injection group then remained within a physiological range indicating a recovery despite a short intracranial hypertensive burst, suggesting that CA was not affected by a pure volume effect beyond the hyperacute phase. A short impairment of PRx was also observed in the slow blood injection group upon completion of the injection. However, PRx returned to baseline and seemed to be unaffected throughout the remaining observation period shortly thereafter.

In contrast, only the rapid blood injection group was characterized by secondary and sustained disruption of CA beyond the hyperacute phase, which persisted throughout the observation period, indicating a protracted disturbance as an early and unique characteristic of severe SAH.

To the authors' knowledge, this is the first experimental data on the functionality of CA in the acute phase after SAH, possibly contributing to EBI. Initial and transient disruption of CA immediately after injection was observed in most groups. However, only animals undergoing rapid injection of blood developed secondary and sustained disruption of CA.

Pronounced Neuronal Cell Loss After Rapid Injection

To further investigate the effects of these early physiological parameter changes on parenchymal cell viability, we performed a histological analysis at the end of our observation period of 6 h. Cell death after SAH via apoptosis and necrosis has been described within the first day after insult, and there is mounting evidence that early deleterious mechanisms may begin already within the first hours after ictus. In their endovascular perforation model, Friedrich et al. showed neuronal degeneration as early as 1 h up to 24 h after injury [48]. Activation of apoptotic signaling starts even earlier [14, 48, 49]. Reduced NeuN immunoreactivity is likely to indicate incipient cell death as shown before, and higher ICP values after SAH have been associated with territorial ischemia [49].

In our analysis, we observed decreased immunoreactivity of NeuN 6 h after SAH in the rapid blood injection group in some areas of hippocampus (DG), but not in CA3/CA4, CA1, and cortex. In CA1, NS_1 showed a decreased number of NeuN+ cells compared to slow saline injection and control group, the reason remains unknown. These results may suggest a pronounced neuronal damage associated with higher ICP peak and disturbances of CA, though inconsistence needs to be taken into concern (see limitations). Marbacher et al. reported that EBI (measured via TUNEL and Fluor-Jade positive neurons) in rabbits linearly correlates with CPP decline after 24 h [13], but not with initial ICP peak. They suggest that the critical threshold to trigger EBI lies between 25 and 40% of CPP depletion during the hyperacute phase after SAH. In our setting, CPP minimum of both rapid injection groups was in this range, but only the fastest injection resulted in pronounced neuronal loss [13].

Microglia play a pivotal role in the proinflammatory cytotoxic response after SAH and microglial depletion reduced the amount of neuronal cell death after SAH significantly [50]. The majority of the literature examines microglia after 24 h and later, while data about earlier changes in microglia are scarce. In our model, we detected no significant differences. Staining for cleaved caspase-3, an apoptotic signaling marker, revealed no positive signaling in any group, leaving open the possibility that the time of analysis may yet be too early to detect discernable changes of an already ensuing cascade.

Clinical Translation: Variation of Blood Injection Velocity as a Suitable Model for Heterogeneous Courses of Subarachnoid Hemorrhage?

Clinical presentation and outcome are highly heterogeneous in SAH. Loss of consciousness—most likely due to a dramatic ICP crisis and consecutive, transient perfusion arrest—serves as a clinical marker for EBI [51] and is also associated with a higher risk of developing DCI [52]; poor admission status is an independent predictor for unfavorable neurological outcome in aSAH and naSAH [32, 52]. While hemorrhage volume in admission CT scans can be comparable, loss of consciousness or transient global ischemia are rarely observed in naSAH [52] or in milder aSAH patients, who at the same time carry a considerably better prognosis.

For this reason, we maintained a comparable injection volume, but modified the rate of injection in order to modulate the ensuing ICP crisis. Slower injection lead to a less rapid and less extensive, absolute ICP increase, and this was associated with ameliorated hyperacute alterations of CPP, CBF, and CA. Beyond the hyperacute phase, a comparable CBF compromise was observed for all injection velocities, implying an ICP-independent, acute vasoconstriction as described before and in line with recent clinical findings: Fraggata et al. showed no difference in early cerebral perfusion when comparing patients with aSAH and naSAH within the first 72 h [39].

In our setup, however, only the rapid injection group portrayed persistent disruption of cerebral autoregulation, suggesting a causal relationship between ICP dynamics and integrity of CA, EBI and ultimately outcome. For this reason, we believe that our approach may be a helpful addition to account for the true heterogeneity of SAH.

Limitations

As every animal model has limitations, our injection model may only provide an approximation to the clinical situation regarding the extent of ICP elevation and cerebral perfusion. We decided to use the injection model in order to have full control over hemorrhage volume and velocity. Importantly, we therefore applied additional volume to the intracranial cavity in contrast to e.g. the endovascular perforation model, where the cerebral artery itself is the bleeding source and the systemic circulation transports blood to the subarachnoid space. Therefore, this model might mimic the human disease more sufficiently. Precisely, there may be a short moment in the human disease, where the blood volume of the aneurysm carrying cerebral vessel may drop due to the rupture and further damage may occur either to the subsequent brain parenchyma or even more distant in consequence of the missing blood supply. Indeed, early infarctions at time point of presentation to the hospital after SAH exist; but they are rather seldom and not limited to the aneurysm carrying vessel territory [53]. We postulate, that the Cushing reflex or collateral circulation may lead to an immediate compensation of the potential deficiency of cerebral intravascular blood volume.

To what extent existing animal models correspond to the actual human disease regarding the ICP increase remains unclear. In practice, patients arrive with a delay of several hours in a specialized cerebrovascular center, prohibiting ICP measurement in the first critical minutes or even hours.

We believe that our model by default can only provide an extrapolated approximation of changes during hyperacute

SAH, but at the same allows for important modifications to study multiparametric influences. Our findings support a possible relationship between bleeding velocity and the dynamics of ICP elevation in the first minutes and therefore a possible explanation to the wide variety of clinical courses observed in SAH—be it a hemorrhage from a small or large aneurysm or even a venous tear.

As mentioned above, generalization of our results regarding neuronal cell loss and inflammation is hampered as only some regions of the hippocampus were affected. Importantly, the choice of SAH plays a part in a different emphasis of neuronal cell death [49, 54]. Using the intracisternal injection model could explain differences in extent and distribution of neuronal cell loss compared to other results [9, 54]. We cannot exclude a sample size bias due to small number of animals used for histological analysis. Furthermore, a possible neuroprotective effect due to ongoing prolonged anesthesia may explain the comparably small neuronal cell damage, as well as the fact that hypoperfusion below the ischemic threshold was only short and transient, followed by timely recovery above the ischemic threshold, prohibiting accentuated apoptosis and cell death.

Due to a comparatively high dropout, our study was underpowered to reliably assess group differences in immunofluorescence properties. Longer-term evaluation of the animals was prohibited as the invasiveness of our monitoring (including preparation of cranial window, invasive blood pressure and ICP measurement) precluded a post-surgical recovery period. Further studies using a chronic experimental setting with only short-term anesthesia for SAH induction, variable blood injection velocities and fluid composition will show whether the here described differences in the acute changes in ICP and blood perfusion will have differential impact on the clinical outcome and behavior as well as brain lesion assessment at later time points.

Conclusion

With tiered injection velocities to emulate different hemorrhage dynamics in SAH, characteristic alterations of blood, intracranial and perfusion pressure were observed in the acute phase. Prolonged hypoperfusion was observed at all blood injection velocities, but only rapid injection of blood resulted in a severe and rapid intracranial hypertensive crisis, prolonged impairment of cerebral autoregulation and pronounced neuronal cell loss. Slower injection velocity was associated with ameliorated hyperacute changes and preservation of CA without neuronal loss, while injection of normal saline alone failed to trigger any longer lasting, acute alterations.

Compliance with Ethical Standards

Conflict Interests The authors declare that there is no conflict of interest.

References

1. Macdonald RL, Schweizer TA. Spontaneous subarachnoid haemorrhage. Lancet. 2017;389(10069):655–66.

2. Vergouwen MD, Vermeulen M, van Gijn J, Rinkel GJ, Wijdicks EF, Muizelaar JP, et al. Definition of delayed cerebral ischemia after aneurysmal subarachnoid hemorrhage as an outcome event in clinical trials and observational studies: proposal of a multidisciplinary research group. Stroke. 2010;41(10):2391–5.

3. Schubert GA, Seiz M, Hegewald AA, Manville J, Thome C. Acute hypoperfusion immediately after subarachnoid hemorrhage: a xenon contrast-enhanced CT study. J Neurotrauma. 2009;26(12): 2225–31.

4. Schubert GA, Seiz M, Hegewald AA, Manville J, Thome C. Hypoperfusion in the acute phase of subarachnoid hemorrhage. Acta Neurochir Suppl. 2011;110(Pt 1):35–8.

5. Westermaier T, Jauss A, Eriskat J, Kunze E, Roosen K. Acute vasoconstriction: decrease and recovery of cerebral blood flow after various intensities of experimental subarachnoid hemorrhage in rats. J Neurosurg. 2009;110(5):996–1002.

6. Westermaier T, Jauss A, Eriskat J, Kunze E, Roosen K. Time-course of cerebral perfusion and tissue oxygenation in the first 6 h after experimental subarachnoid hemorrhage in rats. J Cereb Blood Flow Metab. 2009;29(4):771–9.

7. Bederson JB, Levy AL, Ding WH, Kahn R, DiPerna CA, Jenkins AL 3rd, et al. Acute vasoconstriction after subarachnoid hemorrhage. Neurosurgery. 1998;42(2):352–60 discussion 60-2.

8. Chen S, Feng H, Sherchan P, Klebe D, Zhao G, Sun X, et al. Controversies and evolving new mechanisms in subarachnoid hemorrhage. Prog Neurobiol. 2014;115:64–91.

9. Sehba FA, Hou J, Pluta RM, Zhang JH. The importance of early brain injury after subarachnoid hemorrhage. Prog Neurobiol. 2012 Apr;97(1):14–37.

10. Foreman B. The pathophysiology of delayed cerebral ischemia. J Clin Neurophysiol. 2016;33(3):174–82.

11. Rouchaud A, Lehman VT, Murad MH, Burrows A, Cloft HJ, Lindell EP, et al. Nonaneurysmal perimesencephalic hemorrhage is associated with deep cerebral venous drainage anomalies: a systematic literature review and meta-analysis. AJNR Am J Neuroradiol. 2016;37(9):1657–63.

12. Suwatcharangkoon S, Meyers E, Falo C, Schmidt JM, Agarwal S, Claassen J, et al. Loss of consciousness at onset of subarachnoid hemorrhage as an important marker of early brain injury. JAMA Neurol. 2016;73(1):28–35.

13. Marbacher S, Neuschmelting V, Andereggen L, Widmer HR, von Gunten M, Takala J, et al. Early brain injury linearly correlates with reduction in cerebral perfusion pressure during the hyperacute phase of subarachnoid hemorrhage. Intensive Care Med Exp. 2014;2(1):30.

14. Prunell GF, Svendgaard NA, Alkass K, Mathiesen T. Delayed cell death related to acute cerebral blood flow changes following subarachnoid hemorrhage in the rat brain. J Neurosurg. 2005;102(6):1046–54.

15. Santos GA, Petersen N, Zamani AA, Du R, LaRose S, Monk A, et al. Pathophysiologic differences in cerebral autoregulation after subarachnoid hemorrhage. Neurology. 2016;86(21):1950–6.

16. Budohoski KP, Czosnyka M, Smielewski P, Kasprowicz M, Helmy A, Bulters D, et al. Impairment of cerebral autoregulation predicts delayed cerebral ischemia after subarachnoid hemorrhage: a prospective observational study. Stroke. 2012;43(12):3230–7.

17. Jaeger M, Soehle M, Schuhmann MU, Meixensberger J. Clinical significance of impaired cerebrovascular autoregulation after severe aneurysmal subarachnoid hemorrhage. Stroke. 2012;43(8):2097–101.

18. Budohoski KP, Czosnyka M, Kirkpatrick PJ, Smielewski P, Steiner LA, Pickard JD. Clinical relevance of cerebral autoregulation following subarachnoid haemorrhage. Nat Rev Neurol. 2013;9(3):152–63.

19. Schmieder K, Moller F, Engelhardt M, Scholz M, Schregel W, Christmann A, et al. Dynamic cerebral autoregulation in patients with ruptured and unruptured aneurysms after induction of general anesthesia. Zentralblatt fur Neurochirurgie. 2006;67(2):81–7.

20. Jaeger M, Schuhmann MU, Soehle M, Nagel C, Meixensberger J. Continuous monitoring of cerebrovascular autoregulation after subarachnoid hemorrhage by brain tissue oxygen pressure reactivity and its relation to delayed cerebral infarction. Stroke. 2007;38(3):981–6.

21. Kilkenny C, Browne WJ, Cuthill IC, Emerson M, Altman DG. Improving bioscience research reporting: the ARRIVE guidelines for reporting animal research. PLoS Biol. 2010;8(6):e1000412.

22. Schubert GA, Poli S, Mendelowitsch A, Schilling L, Thome C. Hypothermia reduces early hypoperfusion and metabolic alterations during the acute phase of massive subarachnoid hemorrhage: a laser-Doppler-flowmetry and microdialysis study in rats. J Neurotrauma. 2008;25(5):539–48.

23. Steimers A, Gramer M, Takagaki M, Graf R, Lindauer U, Kohl-Bareis M. Simultaneous imaging of cortical blood flow and haemoglobin concentration with LASCA and RGB reflectometry. Adv Exp Med Biol. 2013;789:427–33.

24. Sugawara T, Ayer R, Jadhav V, Zhang JH. A new grading system evaluating bleeding scale in filament perforation subarachnoid hemorrhage rat model. J Neurosci Methods. 2008;167(2):327–34.

25. Schneider CA, Rasband WS, Eliceiri KW. NIH Image to ImageJ: 25 years of image analysis. Nat Methods. 2012;9(7):671–5.

26. Czosnyka M, Smielewski P, Kirkpatrick P, Laing RJ, Menon D, Pickard JD. Continuous assessment of the cerebral vasomotor reactivity in head injury. Neurosurgery. 1997;41(1):11–7 discussion 7-9.

27. Donnelly J, Budohoski KP, Smielewski P, Czosnyka M. Regulation of the cerebral circulation: bedside assessment and clinical implications. Crit Care. 2016;20(1):129.

28. Sanchez-Porras R, Santos E, Czosnyka M, Zheng Z, Unterberg AW, Sakowitz OW. 'Long' pressure reactivity index (L-PRx) as a measure of autoregulation correlates with outcome in traumatic brain injury patients. Acta Neurochir. 2012;154(9):1575–81.

29. Salary M, Quigley MR, Wilberger JE Jr. Relation among aneurysm size, amount of subarachnoid blood, and clinical outcome. J Neurosurg. 2007;107(1):13–7.

30. Konczalla J, Schmitz J, Kashefiolasl S, Senft C, Seifert V, Platz J. Non-aneurysmal subarachnoid hemorrhage in 173 patients: a prospective study of long-term outcome. Eur J Neurol. 2015;22(10):1329–36.

31. Raya A, Zipfel GJ, Diringer MN, Dacey RG Jr, Derdeyn CP, Rich KM, et al. Pattern not volume of bleeding predicts angiographic vasospasm in nonaneurysmal subarachnoid hemorrhage. Stroke. 2014;45(1):265–7.

32. Kapadia A, Schweizer TA, Spears J, Cusimano M, Macdonald RL. Nonaneurysmal perimesencephalic subarachnoid hemorrhage: diagnosis, pathophysiology, clinical characteristics, and long-term outcome. World Neurosurg. 2014;82(6):1131–43.

33. Dickinson CJ. Reappraisal of the Cushing reflex: the most powerful neural blood pressure stabilizing system. Clin Sci. 1990;79(6):543–50.

34. Sorrentino E, Diedler J, Kasprowicz M, Budohoski KP, Haubrich C, Smielewski P, et al. Critical thresholds for cerebrovascular reactivity after traumatic brain injury. Neurocrit Care. 2012;16(2):258–66.

35. Bijlenga P, Czosnyka M, Budohoski KP, Soehle M, Pickard JD, Kirkpatrick PJ, et al. "Optimal cerebral perfusion pressure" in poor grade patients after subarachnoid hemorrhage. Neurocrit Care. 2010;13(1):17–23.

36. Ebel H, Rust DS, Leschinger A, Ehresmann N, Kranz A, Hoffmann O, et al. Vasomotion, regional cerebral blood flow and intracranial pressure after induced subarachnoid haemorrhage in rats. Zentralblatt fur Neurochirurgie. 1996;57(3):150–5.

37. Steiner L, Lofgren J, Zwetnow NN. Lethal mechanism in repeated subarachnoid hemorrhage in dogs. Acta Neurol Scand. 1975;52(4):268–93.

38. Lee JY, Sagher O, Keep R, Hua Y, Xi G. Comparison of experimental rat models of early brain injury after subarachnoid hemorrhage. Neurosurgery. 2009;65(2):331–43 discussion 43.

39. Fragata I, Canto-Moreira N, Canhao P. Comparison of cerebral perfusion in perimesencephalic subarachnoid hemorrhage and aneurysmal subarachnoid hemorrhage. Neuroradiology. 2018;60(6):609–16.

40. Bederson JB, Germano IM, Guarino L. Cortical blood flow and cerebral perfusion pressure in a new noncraniotomy model of subarachnoid hemorrhage in the rat. Stroke. 1995;26(6):1086–91 discussion 91-2.

41. Ansar S, Edvinsson L. Equal contribution of increased intracranial pressure and subarachnoid blood to cerebral blood flow reduction and receptor upregulation after subarachnoid hemorrhage. Laboratory investigation. J Neurosurg. 2009 Nov;111(5):978–87.

42. Boedtkjer E. Acid-base regulation and sensing: accelerators and brakes in metabolic regulation of cerebrovascular tone. J Cereb Blood Flow Metab. 2017:271678X17733868.

43. Schain AJ, Melo-Carrillo A, Strassman AM, Burstein R. Cortical spreading depression closes paravascular space and impairs

glymphatic flow: implications for migraine headache. J Neurosci. 2017;37(11):2904–15.

44. Balbi M, Koide M, Schwarzmaier SM, Wellman GC, Plesnila N. Acute changes in neurovascular reactivity after subarachnoid hemorrhage in vivo. J Cereb Blood Flow Metab. 2015;16.

45. Balbi M, Koide M, Wellman GC, Plesnila N. Inversion of neurovascular coupling after subarachnoid hemorrhage in vivo. J Cereb Blood Flow Metab. 2017:271678X16686595.

46. Springborg JB, Ma X, Rochat P, Knudsen GM, Amtorp O, Paulson OB, et al. A single subcutaneous bolus of erythropoietin normalizes cerebral blood flow autoregulation after subarachnoid haemorrhage in rats. Br J Pharmacol. 2002;135(3):823–9.

47. Yamamoto S, Nishizawa S, Tsukada H, Kakiuchi T, Yokoyama T, Ryu H, et al. Cerebral blood flow autoregulation following subarachnoid hemorrhage in rats: chronic vasospasm shifts the upper and lower limits of the autoregulatory range toward higher blood pressures. Brain Res. 1998;782(1–2):194–201.

48. Friedrich V, Flores R, Sehba FA. Cell death starts early after subarachnoid hemorrhage. Neurosci Lett. 2012;512(1):6–11.

49. Hollig A, Weinandy A, Nolte K, Clusmann H, Rossaint R, Coburn M. Experimental subarachnoid hemorrhage in rats: comparison of two endovascular perforation techniques with respect to success

rate, confounding pathologies and early hippocampal tissue lesion pattern. PLoS One. 2015;10(4):e0123398.

50. Schneider UC, Davids AM, Brandenburg S, Muller A, Elke A, Magrini S, et al. Microglia inflict delayed brain injury after subarachnoid hemorrhage. Acta Neuropathol. 2015;130(2):215–31.

51. Hop JW, Rinkel GJ, Algra A, van Gijn J. Initial loss of consciousness and risk of delayed cerebral ischemia after aneurysmal subarachnoid hemorrhage. Stroke. 1999;30(11):2268–71.

52. Konczalla J, Platz J, Schuss P, Vatter H, Seifert V, Guresir E. Nonaneurysmal non-traumatic subarachnoid hemorrhage: patient characteristics, clinical outcome and prognostic factors based on a single-center experience in 125 patients. BMC Neurol. 2014;14: 140.

53. Shimoda M, Hoshikawa K, Shiramizu H, Oda S, Yoshiyama M, Osada T, et al. Early infarction detected by diffusion-weighted imaging in patients with subarachnoid hemorrhage. Acta Neurochir. 2010;152(7):1197–205.

54. Prunell GF, Mathiesen T, Diemer NH, Svendgaard NA. Experimental subarachnoid hemorrhage: subarachnoid blood volume, mortality rate, neuronal death, cerebral blood flow, and perfusion pressure in three different rat models. Neurosurgery. 2003;52(1):165–75 discussion 75-6.